

CATION ORDERING PATTERN IN AMESITE

STEPHEN H. HALL¹ AND STURGES W. BAILEY

Department of Geology and Geophysics, University of Wisconsin–Madison
Madison, Wisconsin 53706

Abstract—Cation ordering in amesite- $2H_2$ from Antarctica has reduced the true symmetry from the ideal hexagonal space group $P6_3$ to triclinic $P1$. All crystals show 6-fold biaxial twin sectors on (001), and the twinned crystals produce an average diffraction symmetry that is hexagonal. Individual twin sectors cut from the larger aggregate have $2V$ optic angles near 18° , slightly monoclinic unit-cell geometry, and triclinic diffraction symmetry. Structural refinement of an untwinned sector in subgroup symmetry shows nearly complete ordering of Si,Al in tetrahedral sites and of Mg,Al in octahedral sites.

In triclinic symmetry the two layers in the unit cell are no longer equivalent. Tetrahedra lying on the pseudo- 6_3 screw axis are alternately Si-rich and Al-rich in adjacent layers. Of the three octahedral sites in each layer, one is smaller than the other two and is interpreted as Al-rich. The distribution of Al-rich and Mg-rich octahedra violates both the pseudo-3-fold rotation axis within each layer and the pseudo- 6_3 screw axis that relates one layer to the next in the ideal space group. Local charge balance is achieved in adjacent layers by location of all tetrahedral and octahedral Al in lines parallel to X_1 and spaced at intervals of $b/2$. Similar charge balance patterns parallel to X_2 and X_3 are postulated to account for the sector twinning, which has been observed also in amesites from Chester, Massachusetts, USA, Saranovskoye, USSR, and Postmasburg, South Africa.

Key Words—Amesite, Antarctica, Cation Ordering, Twinning.

INTRODUCTION

Amesite is a rare trioctahedral 1:1 layer silicate that is usually found as hexagonal prisms elongated parallel to Z and that has a maximum amount of tetrahedral and octahedral Al-substitution. The only detailed structural study to date is that of Steinfink and Brunton (1956) on amesite from the Saranovskoye chromite deposits, USSR, in which no ordering of tetrahedral or octahedral cations was found in the ideal space group $P6_3$. The authors noted the presence of 6-fold biaxial twin sectors on (001), but attributed the biaxial nature to strain. The stacking sequence of layers in their specimen and in most other specimens described in the literature to date corresponds to that of the $2H_2$ polytype of Bailey (1969), in which there are alternating interlayer shifts of $-b/3$ and $+b/3$ and alternating occupation of the I and II sets of octahedral positions in successive layers.

Hall and Bailey (1976) described amesite crystals from the Dufek Massif in the Pensacola Mountains, Antarctica, that also exhibit 6-fold biaxial twins. The majority of the crystals are of the $2H_2$ polytype. Five $6R_1$ crystals and one $2H_1$ crystal were identified as well. The X-ray intensities given by the twinned $2H_2$ macrocrystals closely approximate hexagonal symmetry, but excised untwinned sectors have triclinic symmetry. This suggests that cation ordering has reduced the sym-

metry from the ideal space group $P6_3$ to the subgroup $P1$. This paper reports the results of refinement of the structure of the Dufek Massif amesite- $2H_2$ in subgroup symmetry.

EXPERIMENTAL

Although many of the crystals exhibit partial randomness in layer stacking, a regularly stacked, twinned crystal was found in which it was possible to excise an untwinned sector (illustrated in Figure 1 of Hall and Bailey, 1976). Hall and Bailey reported refractive indices of $\alpha = 1.5967(5)$, $\beta = 1.5986(5)$, and $\gamma = 1.615(1)$, $2V = 18^\circ$, and an electron microprobe analysis of this material that gives a structural formula of $(Mg_{1.702}Al_{0.951}Fe^{2+}_{0.315}Mn_{0.014}\square_{0.018})(Si_{1.085}Al_{0.915})O_5(OH)_4$ on the basis of seven formula oxygens.

Because of the triclinic symmetry it was decided to refine the structure using an orthohexagonal cell of space group $C1$, rather than the primitive hexagonal cell. Unit-cell dimensions were obtained by least-squares refinement of 15 medium-angle reflections on an automated single crystal diffractometer. The refined values are $a = 5.319(2)$, $b = 9.208(3)$, $c = 14.060(5)$ Å, $\alpha = 90.01(3)^\circ$, $\beta = 90.27(3)^\circ$, and $\gamma = 89.96(3)^\circ$.

Two sets of intensity data were collected. First, seven levels of data incorporating 772 unique reflections were collected by triple-film-pack Weissenberg photography with $CuK\alpha$ radiation for levels $0kl$ through $2kl$ and $h0l$ through $h3l$. Intensities were measured by visual comparison with a triple-film-pack intensity

¹ Present address: DeLamar Silver Mine, Jordan Valley, Oregon 97910.

scale and were corrected for Lp and attenuation factors. After initial refinement with the film data, a second data set of 722 independent reflections was collected on a Syntex $P\bar{1}$ automated single crystal diffractometer using monochromatic $\text{MoK}\alpha$ radiation. It was necessary to collect the second data set using a second untwinned sector excised from the same $2H_2$ crystal because of loss of the first sector. The shape of each sector was approximately an equilateral triangle of sides 0.25 mm and thickness 0.07 mm. The data were collected in the $2\theta:\theta$ variable-scan mode. Two standard reflections were monitored after every 50 reflections to check crystal and electronic stability. Reflections were considered as observed if $I > 2\sigma(I)$ where I was calculated from $I = [S - (B_1 + B_2)/B_r]T_r$, S being the scan count, B_1 and B_2 the background, B_r the ratio of background time to scan time, and T_r the 2θ scan rate in degrees per minute. $\sigma(I)$ was calculated from standard counting statistics. Integrated intensities were corrected for Lp and attenuation factors.

REFINEMENT

The first data set was used for least-squares refinement of positional coordinates using phase angles calculated from the amesite structure of Steinfink and Brunton (1956). Scattering factors from the International Tables for X-ray Crystallography, adjusted for 50% ionization, were used throughout. In order to facilitate convergence, atomic coordinates were moved slightly away from their ideal hexagonal positions. Refinements were attempted with tetrahedra rotated both toward and away from octahedral cations of the same layer. Only the former provided satisfactory refinement. The tetrahedral cation $T(1)$ was kept stationary in order to fix the position of the origin in this noncentrosymmetric structure, and the sense of the Z axis was determined by comparison of F_o and F_c values. Repeated cycles of refinement using unitary weights and varying first the positional atomic coordinates and later the isotropic B values reduced the residual to $R = 13.3\%$. Bond-length calculations indicated ordering of both tetrahedral and octahedral cations, but the results were unsatisfactory in two respects. The isotropic B values varied erratically from atom to atom, and the z coordinates of the apical oxygens in one of the two 1:1 layers appeared unrealistic in terms of the implied sheet thicknesses.

At this stage the second data set was collected from a second untwinned amesite sector, and refinement was continued with this data set until convergence was achieved at $R = 10.9\%$. The results of this stage of refinement were reported in detail by Hall (1974) and in summary form by Bailey (1975).

Later refinement made use of two changes in the second data set.

(1) Data corrected only for Lp effects were used due

Table 1. Atomic parameters for Antarctic amesite.

Atom	x	y	z	B	
$M(1)$	0.1668	0.1710	0.2384	0.48	
$M(2)$	0.6678	0.0013	0.2374	0.77	
$M(3)$	0.6721	0.3372	0.2373	0.64	
$M(11)$	0.3337	0.3359	0.7363	0.41	
$M(22)$	0.3294	0.0003	0.7388	0.74	
$M(33)$	0.8305	0.1650	0.7385	0.60	
$T(1)$	0.0000	0.0000	0.0410	0.44	
$T(2)$	-0.0059	0.3353	0.0416	0.62	
$T(11)$	-0.0117	0.0010	0.5424	0.72	
$T(22)$	0.4900	0.1718	0.5408	0.52	
O	O(1)	0.0122	-0.0072	0.1606	1.10
	O(2)	-0.0152	0.3391	0.1668	0.92
	O(3)	0.0660	0.1658	0.0042	1.87
	O(4)	0.7235	-0.0444	0.0050	1.33
	O(5)	0.7000	0.3852	-0.0012	1.87
	O(11)	-0.0144	-0.0089	0.6652	0.73
	O(22)	0.4856	0.1791	0.6613	0.61
	O(33)	0.2819	0.0546	0.5041	1.35
	O(44)	0.4118	0.3305	0.4989	1.63
	O(55)	0.7728	0.1266	0.5048	1.73
	OH	OH(1)	0.5090	0.1802	0.1639
OH(2)		0.3242	-0.0060	0.3088	0.67
OH(3)		0.3598	0.3393	0.3061	1.12
OH(4)		0.8212	0.1812	0.3080	1.40
OH(11)		0.0136	0.3329	0.6637	1.35
OH(22)		0.6484	0.3322	0.8066	1.31
OH(33)		0.6743	-0.0116	0.8076	1.20
OH(44)		0.1741	0.1800	0.8077	0.91

to discovery that the theoretical absorption program had not been giving correct results. The linear absorption coefficient for $\text{MoK}\alpha$ for this composition is small ($\mu_{\text{Mo}} = 14.9$), but it is believed that lack of correction for the platy shape of the crystal may have caused some of the variability noted in the final results. Nevertheless, refinement tests both before and after change (2) noted below consistently gave more realistic and consistent values using the data as corrected only for Lp effects.

(2) Weissenberg film photographs of the second crystal after automated data collection showed a doubling and streaking of several low θ reflections that had not been noted previously. It is believed that this distortion developed during data collection due to strain caused by shrinkage of the solvent-based mounting glue. Forty-three $k \neq 3n$ reflections for which the distortion was evident on the films were removed from the data set, and separate scale factors were introduced for $k = 3n$ and $k \neq 3n$ reflections in case other $k \neq 3n$ reflections had been affected also.

Further least-squares refinement with the remaining 679 reflections proceeded smoothly with unit weights and isotropic B values to a residual of 7.9%. Electron-

Table 2. Interatomic bond lengths in Å for Antarctic amesite.

Tetrahedron T(1)				Tetrahedron T(2)			
O(1)	1.684	O(1)–O(3)	2.732	O(2)	1.761	O(2)–O(3)	2.822
O(3)	1.651	O(4)	2.689	O(3)	1.691	O(4)	2.822
O(4)	1.606	O(5)	2.679	O(4)	1.729	O(5)	2.831
O(5)	1.614	O(3)–O(4)	2.659	O(5)	1.735	O(3)–O(4)	2.797
Mean	1.639	O(5)	2.682	Mean	1.729	O(5)	2.805
		O(4)–O(5)	2.618			O(4)–O(5)	2.860
		Mean	2.676			Mean	2.823
Tetrahedron T(11)				Tetrahedron T(22)			
O(11)	1.729	O(11)–O(33)	2.826	O(22)	1.695	O(22)–O(33)	2.711
O(33)	1.727	O(44)	2.793	O(33)	1.629	O(44)	2.702
O(44)	1.733	O(55)	2.811	O(44)	1.629	O(55)	2.728
O(55)	1.710	O(33)–O(44)	2.854	O(55)	1.643	O(33)–O(44)	2.634
Mean	1.725	O(55)	2.787	Mean	1.649	O(55)	2.695
		O(44)–O(55)	2.826			O(44)–O(55)	2.686
		Mean	2.816			Mean	2.693
Octahedron				Octahedron			
M(1)	M(2)	M(3)		M(11)	M(22)	M(33)	
O(1)	2.135	2.132	1.982	O(11)	1.924	2.099	2.077
O(2)	2.083	2.039	1.940	O(22)	1.964	2.145	2.131
OH(1)	2.106	2.118	1.975	OH(11)	1.982	2.112	2.112
OH(2)	2.080	2.091	1.934	OH(22)	1.941	2.060	2.057
OH(3)	2.086	2.047	1.926	OH(33)	1.924	2.072	2.071
OH(4)	2.088	2.095	1.916	OH(44)	1.949	2.089	2.072
Mean	2.096	2.087	1.946	Mean	1.947	2.096	2.087
			Mean unshared anion edges				
	3.180	3.161	2.879		2.882	3.179	3.159
			Mean shared anion edges				
	2.733	2.726	2.618		2.620	2.733	2.726
			Interlayer bonds				
		OH(2)–O(33)	2.812			OH(22)–O(5)	2.758
		OH(3)–O(44)	2.725			OH(33)–O(4)	2.804
		OH(4)–O(55)	2.825			OH(44)–O(3)	2.827
		Mean	2.787			Mean	2.796

One standard deviation for all bond lengths is 0.02 Å.

density difference maps were flat at the atomic positions but indicated anisotropic thermal motion, which prohibited location of the hydrogen atoms. One cycle of anisotropic refinement reduced the residual to 4.6%, but anisotropic refinement was discontinued because many atoms were not positive-definite. The major axes of the thermal ellipsoids were perpendicular to the layers. Scattering factor tables appropriate to 50% ionization were used throughout and were adjusted for the indicated ordering patterns. No change in ordering pattern was found throughout the several stages of refinement, but there was a significant improvement in consistency of bond lengths and temperature factors during the last stage of refinement. The final atomic coordinates, bond lengths, and other important structural features are reported in Tables 1–3. A list of observed and calculated structure amplitudes may be obtained from the second author (SWB) upon request.

CATION ORDERING

The most interesting feature of the amesite structure is its unusual pattern of ordering of tetrahedral and octahedral cations. The same ordering pattern was found as a result of refinement of both data sets, and it is this pattern that causes the reduction in symmetry from $P6_3$ to $P1$ (or $C1$ as oriented here). It should be noted that even in the ideal hexagonal space group there are two unique tetrahedra in each layer, so that a tetrahedral cation ordering pattern preserving the identity of the 6_3 axis is theoretically possible but is not observed. In the lower symmetry $C1$ the two layers in the unit cell are no longer equivalent. Tetrahedra lying on the pseudo- 6_3 axis in fact are not identical, but are alternately Si-rich [$T(1)$] and Al-rich [$T(11)$] in adjacent layers. Of the three octahedra in each layer, one is smaller than the other two and is interpreted as Al-rich. These are $M(3)$ in the first layer and $M(11)$ in the second layer (Table

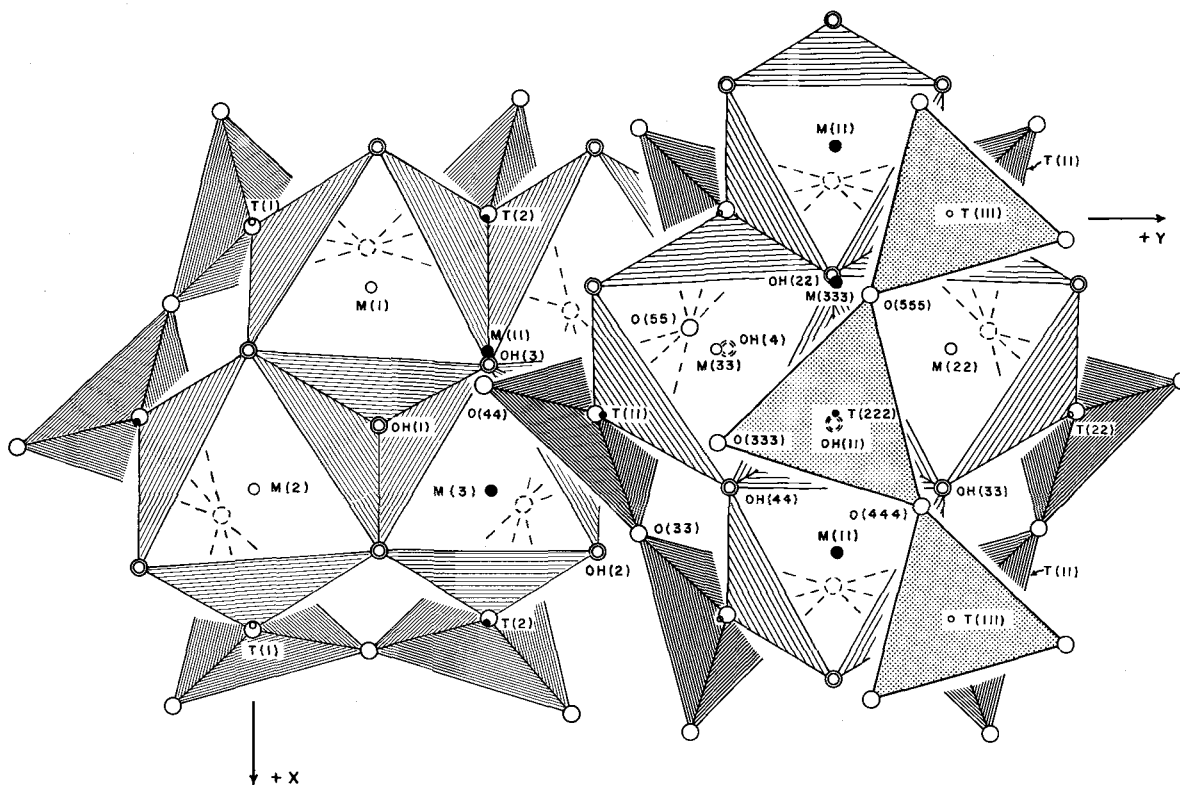


Figure 1. Diagrammatic view of amesite- $2H_2$ structure. For clarity, the structure is cut away so that layer 1 is shown on the left side and layer 2 on the right side with the bases of three tetrahedra (stippled pattern) from layer 3 superimposed. Cation $M(11)$ from layer 2 on the left and $M(333)$ from layer 3 on the right are shown without their enclosing octahedra. Al is shown in solid circles.

2). The distribution of Al-rich and Mg-rich octahedra (Figure 1) violates both the pseudo-3-fold rotation axes within each layer and the pseudo- 6_3 axes that relate one layer to the next in the ideal space group.

The mean tetrahedral bond lengths of 1.639, 1.729, 1.725, and 1.649 Å (Table 2) indicate that tetrahedral ordering of Si, Al is substantial but incomplete. Because of the lack of well-refined structures no determinative equation relating mean $T-O$ bond lengths to Si, Al compositions has been proposed for 1:1 layer silicates. Using 1.619 Å as the mean of values recorded for Si-O in dickite and nacrite and the grand mean of 1.685 Å observed in this study for amesite, a predicted mean value for $Al^{IV}-O$ of 1.764 Å is obtained and a predicted linear equation of $\overline{T-O} = 1.619 \text{ Å} + 0.145[x_{Al}/(x_{Al} + x_{Si})]$. This equation gives values for Al^{IV} of 0.14, 0.76, 0.73, and 0.21, respectively, for $T(1)$, $T(2)$, $T(11)$, and $T(22)$. Maximum ordering for the indicated microprobe composition would be 0.00 and 0.92.

Octahedral cation ordering also is substantial but incomplete. The four larger octahedra with mean $M-O, OH$ values of 2.096, 2.087, 2.096, and 2.087 Å (Table 2) are interpreted as Mg-rich and the two smaller octahedra ($M(3)$ and $M(11)$) with mean $M-O, OH$ values of 1.946 and 1.947 Å are interpreted as Al-rich. Al^{VI} -

O, OH values in dickite, nacrite, muscovite, and paragonite average 1.920 Å. The observed slightly larger values of 1.946 and 1.947 Å are in accord with the microprobe analysis showing less than 1.0 octahedral Al

Table 3. Important structural features.

α_{tet} (°)	Layer 1: 13.6 Layer 2: 14.5
τ_{tet} (°)	$T(1)$: 109.4 $T(2)$: 108.6 $T(11)$: 109.0 $T(22)$: 109.2
ψ_{oct} (°)	$M(1), M(22)$: 60.8 $M(2), M(33)$: 60.7 $M(3), M(11)$: 58.3
Sheet thickness (Å)	
tetrahedral	2.263
octahedral	2.023
Interlayer separation	2.744

Tetrahedral rotation is calculated from

$$\alpha = \frac{1}{2} |120^\circ - \text{mean } O_b-O_b-O_b \text{ angle}|.$$

Tetrahedral angle is defined as $\tau = O_{ap}-T-O_b$.

The ideal value is 109.47°.

Mean octahedral angle is calculated from

$$\cos \psi = \text{octahedral thickness} / 2(M-O, OH).$$

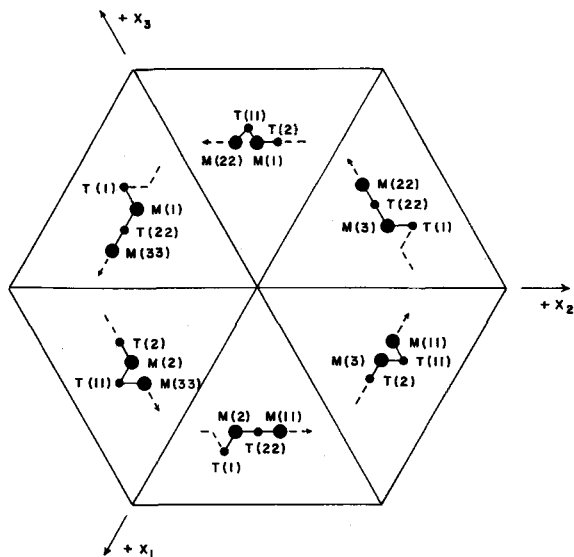


Figure 2. Diagrammatic view of 6-fold sector twinning in amesite with postulated ordered positions of Al atoms, as viewed in projection. Arrow indicates direction of continuation of ordering pattern in the third layer along resultant $-X$ in each sector.

per formula unit and the presence of some larger Fe^{2+} , Mn ions. Least-squares variation of cation multiplicities with program ORFLS indicated similar scattering powers for all octahedral sites, so the Fe^{2+} , Mn, and vacancies are assumed to be distributed randomly over all sites.

Si-rich and Al-rich tetrahedra alternate along lines parallel to Z through each lattice point, thus violating the 6_3 axes of the ideal space group. Si-rich and Al-rich tetrahedra also alternate around the 6-fold rings within each layer. The second unique tetrahedron in each layer lies on a pseudo-3-fold rotation axis, and adjacent layers are shifted by $\pm b/3$ so that these tetrahedra do not superimpose in projection. The Al-rich octahedron $M(3)$ in the first layer is in the C position in the terminology of Bailey (1963, Figure 1) and the Al-rich octahedron $M(11)$ in the second layer is in the A position (after allowance for 180° rotation of octahedra relative to the first layer, which is equivalent to occupation of the alternate set of octahedral positions). This creates a pattern of local charge balance in which all tetrahedral and octahedral Al atoms in adjacent layers are located along slightly zigzag lines parallel to X_1 in projection and spaced at intervals of $b_1/2$ (Figure 1). Thus, from bottom to top in the $-X_1$ direction, Al is located in $T(2)$, $M(3)$, $T(11)$, and $M(11)$. This gives the closest possible approach of the sources of negative and positive charges on the surfaces of adjacent layers that result from the ordered substitution of Al in the tetrahedral and octahedral sheets. But this is not an unique order-

ing pattern. Because of the pseudohexagonal nature of the structure, different ordering patterns can be created in which the zigzag lines of Al atoms are parallel in projection to both the positive and negative directions of X_1 , X_2 , and X_3 . Adoption of these alternate patterns in adjacent sectors is postulated here as the origin of the 6-fold sector twins. We have found twinning of this type to be universal in amesite from Antarctica, as well as in amesites from the Chester emery deposit in Massachusetts, USA, the Saranovskoye chromite deposit in the North Urals, USSR, and the Postmasburg Mn-ores near Gloucester, South Africa. Figure 2 shows the six ordering patterns and their postulated distribution in a twinned crystal. Optical extinction directions would be parallel and perpendicular to the line of ordered Al in each sector. In all six patterns Si and Al alternate along the Z axis on the pseudo- 6_3 screw axis and, considering all six sectors together, the Al would be distributed equally over the four tetrahedral sites and the six octahedral sites of the 2-layer structure.

Serna *et al.* (1977) concluded from study of infrared spectra that some synthetic and natural amesites, including that from Chester, Massachusetts, have an ordered distribution of tetrahedral cations. An infrared pattern of the Antarctic amesite, kindly run and interpreted by J. L. White of Purdue University, is in accord with their criteria for an ordered cation distribution. Serna *et al.* considered other amesite specimens, including that from Saranovskoye, North Urals, to be disordered. Our observation of biaxial optics and twinning in the Urals crystals, however, is interpreted here by analogy with the results for the Antarctica specimen as evidence of ordering. A more complex twinning behavior was noted in the Urals crystals than in those from other localities, in that polysynthetic twin lamellae parallel to the prism edges are present in some crystals in addition to the 6-fold sector twins. This difference in twinning may result from a difference in ordering pattern. The $2H_2$ structure does permit additional ordering patterns with local charge balance, although with geometries in which the Al atoms are not arranged in the slightly zigzag lines illustrated in Figure 2. A structural refinement to determine the actual cation distribution of a $2H_2$ amesite from the Urals locality is in progress.

INTERLAYER BONDING

The basal oxygens of the second layer [O(33), O(44), and O(55)] are positioned symmetrically relative to the surface hydroxyls [OH(2), OH(3), and OH(4)] of the layer below, and these basal oxygens move closer to the surface hydroxyls by means of tetrahedral twist (Figure 1). The interlayer separations are short because of the large positive and negative charges on adjacent surfaces due to octahedral and tetrahedral substitutions. The hydrogen bond contact O(44)–OH(3) of

2.725 Å is especially short because OH(3) is the only surface hydroxyl located so that its movement to shorten its bond to Al in $M(3)$ also brings it closer to its basal oxygen neighbor O(44). Because of the location of Al in $M(11)$ of the second layer, tetrahedra $T(11)$ and $T(22)$ of that layer tilt towards one another to allow a shortened octahedral lateral edge around $M(11)$, thereby causing a downward buckling of the bridging basal oxygen O(44). The surface hydroxyl OH(3) is also depressed, so that there is a keying together of the two layers at the site of this most favorable interlayer bond O(44)–OH(3).

Because of the adoption of the alternate set of octahedral positions in the third layer and location of Al in $M(333)$, equivalent to $M(3)$ of the first layer, the topological setting of the most favorable interlayer bond between layers two and three is slightly different than between layers one and two. Movement of OH(22) towards octahedral Al in $M(11)$ of layer two now is away from basal oxygen O(555) of layer three, instead of towards it, thereby increasing the interlayer O–OH bond by 0.03 Å. The keying together of O(555) and OH(22) is the same as for O(44) and OH(3); however, as a result of the location of Al in $M(333)$ of the third layer with a consequent tilting of $T(111)$ and $T(222)$ and a downward buckling of O(555) and OH(22). This keying effect due to ordering is believed to be a positive factor in influencing the regularity of stacking of layers in amesite and in its resultant stability.

OTHER STRUCTURAL FEATURES

The tetrahedra in this structure are rotated in the (001) plane by an average value of 14.0° so that the basal oxygens move in a direction toward the octahedral cations in the same layer. This also is in the direction that will shorten the interlayer hydrogen bonds between the basal oxygens and surface hydroxyl groups of the adjacent layer. The direction of tetrahedral rotation is opposite to that found by Steinfink and Brunton (1956) in their study of Saranovskoye amesite, but it should be remembered that only a small amount of trial-and-error refinement was performed in their study and that the space group used was incorrect.

Tetrahedral tilting combined with tetrahedral and

octahedral ordering has displaced the tetrahedral apical oxygens and distorted the tetrahedral angles (Tables 2, 3). The tetrahedral sheet thicknesses, however, are comparable with those of many other layer silicates. The octahedral sheet thicknesses, on the other hand, are unusually small and are comparable to those in dioctahedral dickite and nacrite. All of the octahedra are flattened, as indicated by the ψ values in Table 3, and the two large octahedra in each layer are flattened most severely ($\psi = 60.7^\circ$ and 60.8°) in order to fit onto the smaller Al-rich octahedron ($\psi = 58.3^\circ$). An undistorted octahedron would have $\psi = 54.7^\circ$. The combination of thin octahedral sheets and short interlayer separations leads to a total layer thickness of only 7.03 Å.

ACKNOWLEDGMENTS

This research was supported in part by the Earth Sciences Section, National Science Foundation, grant EAR76-06620, and in part by the Petroleum Research Fund, administered by the American Chemical Society, grant 8425-AC2. The Antarctica amesite crystals were provided by J. C. Behrendt of the U.S. Geological Survey. J. L. White of Purdue University kindly ran an infrared pattern of the Antarctic amesite and provided crystals from Saranovskoye. The Geological Survey of South Africa, through J. le Roux, provided crystals from Postmasburg. S. J. Guggenheim provided advice on computing procedures.

REFERENCES

- Bailey, S. W. (1963) Polymorphism of the kaolin minerals: *Amer. Mineral.* **48**, 1196–1209.
- Bailey, S. W. (1969) Polytypism of trioctahedral 1:1 layer silicates: *Clays & Clay Minerals* **17**, 355–371.
- Bailey, S. W. (1975) Cation ordering and pseudosymmetry in layer silicates: *Amer. Mineral.* **60**, 175–187.
- Hall, S. H. (1974) The triclinic crystal structure of amesite: M.S. thesis, Univ. Wisconsin–Madison, 63 pp.
- Hall, S. H. and Bailey, S. W. (1976) Amesite from Antarctica: *Amer. Mineral.* **61**, 497–499.
- Serna, C. J., Velde, B. D., and White, J. L. (1977) Infrared evidence of order-disorder in amesites: *Amer. Mineral.* **62**, 296–303.
- Steinfink, H. and Brunton, G. (1956) The crystal structure of amesite: *Acta Crystallogr.* **9**, 487–492.

(Received 8 January 1979; accepted 24 February 1979)

Резюме—Катионное упорядочивание в амезите- $2H_2$ из Антарктики уменьшает истинную симметрию от идеальной гексагональной пространственной группы $P6_3$ до триклиновой $P1$. Все кристаллы проявляют 6-кратные двусосные двойниковые секторы на (001), а двойниковые кристаллы дают среднюю дифракционную гексагональную симметрию. Индивидуальные двойниковые секторы, отделенные от крупного агрегата, имеют оптические углы $2V$, около 18° , слегка моноклиническую геометрию элементарной ячейки и триклиновую дифракционную симметрию. Структурное совершенство недвойникового сектора в симметрии подгруппы показывает почти полное упорядочение Si, Al в тетраэдрических участках и Mg, Al в октаэдрических участках.

В триклиновой симметрии два слоя в элементарной ячейке больше не являются эквивалентными. В тетраэдрическом залегании на псевдо- 6_2 винтовых осях смежные слои попеременно обогащены Si и Al. Из трех октаэдрических участков в каждом слое один меньше двух других и определяется как обогащенный Al. Распределение обогащенных Al и Mg октаэдров нарушает псевдо-3-кратные оси вращения в каждом слое и псевдо- 6_3 винтовые оси, что определяет соотно-

шение одного слоя со следующим в идеальной пространственной группе. Местное равновесие заряда достигается в смежных слоях благодаря расположению всего тетраэдрического и октаэдрического Al на линиях, параллельных X_1 и в интервалах $b_1/2$. Аналогичное равновесие зарядов в линиях, параллельных X_2 и X_3 постулируется для двойниковых секторов, которые наблюдались также в амезитах из Честер, Массачусетс, США; Сарановское, СССР; и Постмасбург, Южная Африка.

Résumé—Kationenarrangierungen in antarktischen Amesit- $2H_2$ hat die wahre Symmetrie von der idealen hexagonalen Raumgruppe $P6_3$ zur triklinischen $P1$ reduziert. Alle Kristalle haben sechsfache biaxiale Zwillingssektoren auf (001) und die Duokristalle produzieren eine hexagonale durchschnittliche Diffraktionsymmetrie. Einzelne Zwillingssektoren, welche von den größeren Aggregaten geschnitten wurden, haben $2V$ optische Winkel von ungefähr 18° , fast monoklinische Einzelzelleometrie und triklinische Diffraktionsymmetrie. Strukturelle Verfeinerung eines einzelnen Sektors in der Untergruppensymmetrie zeigt fast vollständige Anordnung von Si,Al in tetraedrischen Plätzen und von Mg,Al in oktaedrischen Plätzen.

In triklinischer Symmetrie sind die zwei Schichten in der Einheitszelle nicht mehr equivalent. Tetraedren, die auf der pseudo- 6_3 Schraubenachse liegen, sind in benachbarten Schichten abwechselnd Si und Al reich. Von den drei oktaedrischen Plätzen in jeder Schicht ist einer kleiner als die anderen zwei und sie wird als Al reich interpretiert. Die Verteilung von Al reichen und Mg reichen Oktaedern verstößt sowohl gegen die pseudo-dreifache Drehachse innerhalb jeder Schicht und die pseudo- 6_3 Schraubenachse, die eine Schicht mit der anderen in der idealen Raumgruppe verknüpft. Örtlicher Ladungsausgleich wird in angrenzenden Schichten erreicht, indem alles tetraedrische und oktaedrische Al in Reihen parallel zu X_1 und in Intervallen von $b_1/2$ angelegt wird. Ähnliche Ladungsausgleichsmuster, parallel zu X_2 und X_3 , sind vorgeschlagen worden, um die Zwillingssektoren zu erklären, welche auch in Amesiten von Chester, Massachusetts, USA; Saranovskoye, USSR; und Postmasburg, Südafrika, gefunden wurden.

Résumé—Le rangement de cations dans l'amesite- $2H_2$ de l'Antarctique a réduit la symétrie réelle du groupe d'espace hexagonal idéal $P6_3$ à celui triclinique $P1$. Tous les cristaux montrent des secteurs jumelés à 6 faces sur (001), et les cristaux jumelés produisent une symétrie de diffraction moyenne hexagonale. Des secteurs jumelés individuels coupés du plus grand agrégat ont des angles optiques $2V$ près de 18° , une géométrie de maille légèrement monoclinique, et une symétrie de diffraction triclinique. Le raffinement structural d'un secteur non-jumelé dans la symétrie de sous-groupe montre un rangement presque complet de Si,Al dans les sites tétraédres et de Mg,Al dans les sites octaédres.

En symétrie triclinique, les 2 couches de la maille ne sont plus équivalentes. Les tétraédres sur l'axe de vis pseudo- 6_3 sont alternativement riches en Si et en Al dans des couches adjacentes. Parmi les 3 sites octaédres dans chaque couche, un site est plus petit que les 2 autres, et est interprété comme étant riche en Al. La distribution des octaédres riches en Al et des octaédres riches en Mg viole à la fois l'axe de rotation pseudo-à 3 faces compris dans chaque couche et l'axe de vis pseudo- 6_3 qui rapporte une couche à la suivante dans le groupe d'espace idéal. L'équilibre de charge local est acquis dans des couches adjacentes par l'emplacement de tous les Al tétraédres et octaédres en lignes parallèles à X_1 et espacés à des intervalles de $b_1/2$. Des systèmes similaires d'équilibre de charge parallèles à X_2 et X_3 sont suggérés pour expliquer le jumelage des secteurs, remarqué également dans des amésites de Chester, Massachusetts, USA; de Saranovskoye, URSS; et de Postmasburg, Afrique du Sud.